ACS NUTRITION SCIENCE

pubs.acs.org/ACSNutritionSci

Article

αG-Rutin Mitigates Telomere Attrition and Prevents Cellular Senescence

Takumi Terada, Vinodh J Sahayasheela, Ryohei Noizumi, Akihito Nakanishi, Mahamadou Tandia, and Hiroshi Sugiyama*

Cite This: https://doi.org/10.1021/acsnutrsci.5c00012

Read Online

ACCESS | Metrics & More | Article Recommendations | Supporting Information

ABSTRACT: Reactive oxygen species (ROS) are known to contribute to intracellular oxidative damage, telomere attrition, and the induction of cellular senescence. Although plant-derived polyphenols show promise in mitigating this process, their poor water solubility and bioavailability limit their practical application. To address these limitations, transglycosylated polyphenols have been developed. In this study, we evaluated four transglycosylated polyphenols (αG-Resveratrol, αG-Hesperidin, αG-Naringin, and αG-Rutin) for their capacity to reduce intracellular ROS, prevent telomere attrition, and mitigate cellular senescence. Among them, αG-Rutin exhibited the most potent antioxidant effects *in vitro*. Cellular studies demonstrated that αG-Rutin significantly reduced intracellular ROS and 8-oxoguanine accumulation, attenuating telomere shortening under chronic oxidative stress and replicative aging. Finally, αG-Rutin prevented oxidative stress-induced cellular senescence, suppressing senescence-associated β-galactosidase activity and interleukin-6 secretion. These findings highlight the potential of αG-Rutin as a functional food ingredient to combat telomere attrition, prevent cellular senescence, and promote healthy aging.

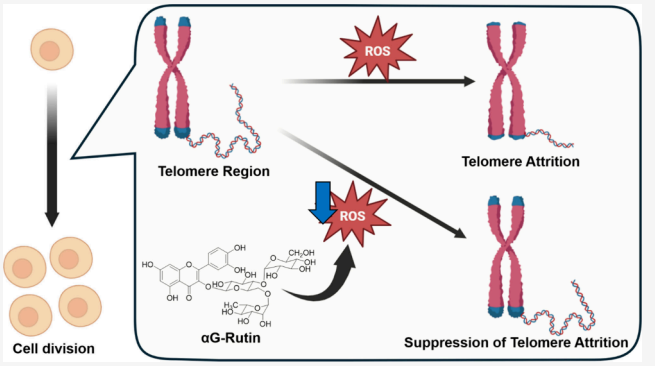

KEYWORDS: *telomere attrition, oxidative stress, cellular senescence, reactive oxygen species (ROS), polyphenols*

1. INTRODUCTION

Cellular aging is characterized by multiple hallmarks, among which telomere attrition is a well-established indicator of cellular aging across various organisms.[1] Telomeres are DNA−protein complexes situated at the termini of chromosomes, comprising a tandem repeat of the sequence TTAGGG, which is bound by a protein complex known as shelterin.[2] These structures are essential for maintaining chromosomal stability and facilitating DNA replication during cell division.[3,4] Progressive telomere shortening is observed with aging, and studies have demonstrated that individuals and mouse models with shorter telomeres tend to exhibit decreased lifespans.[5,6] Further telomere erosion triggers cellular senescence, a state of irreversible growth arrest accompanied by a senescence-associated secretory phenotype (SASP) of secreted pro-inflammatory cytokines that contribute to tissue dysfunction and age-related pathologies.[7,8] Several factors influence telomere shortening during cellular aging, with oxidative DNA damage induced by ROS playing a particularly significant role.[9] Telomeres are sensitive to oxidative stress, a phenomenon termed "TelOxidation" which accelerates telomere erosion. This enhanced susceptibility stems from the intrinsic features of telomeric DNA, which is rich in guanine residues that are more prone to oxidative damage due to their lower oxidation potential.[10,11] Furthermore, DNA repair mechanisms are often less effective in these regions, resulting in the accumulation of oxidative lesions such as 8-oxoG and single-strand breaks.[12,13] In addition, oxidative damage can also promote senescence via telomere-independent mechanisms. Notably, premature senescence is induced by hydrogen peroxide even when telomere length is preserved through telomerase overexpression,[14] and telomeric 8-oxoG formation by itself is sufficient to elicit rapid premature senescence without telomere shortening.[15] Therefore, developing strategies to reduce intracellular ROS and protect cells from oxidative damage is critical for preventing or slowing telomere shortening and cellular senescence.

In this context, several studies have highlighted the potential of antioxidants for telomere protection.[16] Notably, polyphenols, plant-derived antioxidants with a longstanding history of dietary use, are considered safe and suitable as functional food

Received: July 19, 2025
Revised: October 6, 2025
Accepted: October 24, 2025

ingredients.[17] However, polyphenols typically exhibit low water solubility, which presents challenges for their incorporation as food additives and results in limited absorption and bioavailability in the human body.[18] To overcome these limitations, efforts have been made to enhance water solubility and bioavailability by conjugating polyphenols with sugars to form glycosides.[19] For instance, αG-Rutin, formed through the enzymatic attachment of α-glucose to Rutin, demonstrates approximately 30,000 times higher water solubility, along with reduced cellular toxicity and improved intestinal absorption.[20−22] However, the intracellular antioxidant activity of these glycosides, particularly their effectiveness against ROS and their protective effects on intracellular oxidative damage, telomere attrition, and cellular senescence remains to be elucidated.

In this study, we assessed the antioxidant activity of four polyphenols (Resveratrol, Hesperidin, Naringin, and Rutin) along with their transglycosylated derivatives (αG-Resveratrol, αG-Hesperidin, αG-Naringin, and αG-Rutin). Among these, αG-Rutin exhibited the most potent antioxidant activity *in vitro*. Subsequently, we confirmed its intracellular antioxidant effects and its capacity to inhibit the formation of the common DNA lesion, 8-oxoG. Furthermore, αG-Rutin attenuated telomere attrition under chronic oxidative stress and replicative aging by decreasing intracellular ROS levels and DNA damage. Importantly, αG-Rutin also prevents the onset of cellular senescence, suppressing both senescence-associated β-galactosidase activity and pro-inflammatory SASP factor, supporting its potential role in telomere protection and healthy aging.

2. MATERIALS AND METHODS

2.1. Chemicals. Rutin, αG-Rutin, Resveratrol, αG-Resveratrol, Hesperidin, αG-Hesperidin, Naringin, and αG-Naringin were provided by the Toyo Sugar Refining Co., Ltd. (Tokyo, Japan);[23−25] ABTS (2,2′-azino-bis(3-ethylbenzothiazoline-6-sulfonic acid)), DMSO (dimethyl sulfoxide), hydrogen peroxide, NBT (Nitro blue tetrazolium), NADH (nicotinamide adenine dinucleotide, reduced form), thiobarbituric acid, PMS (phenazine methyl sulfate), 2-deoxy-D-ribose, ascorbic acid, BHT (2,6-Di*tert*-butyl-*p*-cresol), and DCFDA (2′,7′-dichlorodihydrofluorescein diacetate) were from TCI (Tokyo, Japan); Dipotassium hydrogen phosphate, potassium dihydrogen phosphate, ascorbic acid, and trichloroacetic acid were from Wako (Osaka, Japan); $FeCl_3$ (iron(III) chloride) and $K_2S_2O_8$ (potassium persulfate) were purchased from Sigma-Aldrich (St. Louis, Missouri, America); EDTA (ethylendiaminetetraacetic acid) was purchased from nacalai tesque (Kyoto, Japan)

2.2. DPPH Assay. The radical scavenging activity of the compounds was assessed using a DPPH (2,2-diphenyl-1-picrylhydrazyl) antioxidant assay kit (Dojindo, Kumamoto, Japan), following the manufacturer's instructions. Briefly, 100 μL of DPPH solution prepared in ethanol was mixed with 80 μL of assay buffer from the kit and 20 μL of the sample solution in a clear 96-well microplate. The reaction mixture was incubated in the dark at 25 °C for 30 min. After incubation, the absorbance was measured at 517 nm using a SpectraMax M2e microplate reader (Molecular Devices). Test sample solutions were prepared with assay buffer to final concentrations ranging from 19.6 to 2500 μg/mL. Control consisted of 20 μL of DMSO instead of the sample solution, and the blank consisted of 20 μL of ethanol instead of the sample solution. The radical scavenging activity was calculated using the following equation:

$$\text{scavenging activity}(\%) = 100 \times (A_{\text{DMSO}} - A_{\text{sample}})/(A_{\text{DMSO}} - A_{\text{blank}})$$

2.3. ABTS Assay. The radical scavenging activity of the compounds under hydrophilic conditions was measured using ABTS radical scavenging assay, according to a previously reported method.[26] An aqueous solution containing 7 mM ABTS and 2.45 mM potassium persulfate ($K_2S_2O_8$) was prepared and incubated in the dark at 25 °C for 16 h to generate the ABTS radical cation ($ABTS^{\bullet+}$). The resulting solution was diluted with ethanol to achieve an initial absorbance of approximately 0.7, measured at 734 nm. In a 96-well clear microplate, 290 μL of the diluted $ABTS^{\bullet+}$ solution was mixed with 10 μL of sample (Rutin or αG-Rutin), resulting in final concentrations ranging from 1.56 to 400 μM. For control, 10 μL of DMSO was used instead of the sample, and for blank, 10 μL of ethanol was added in place of the sample solution. After incubation in the dark at 25 °C for 7 min, the absorbance was measured at 734 nm using a SpectraMax M2e microplate reader (Molecular Devices). Radical scavenging activity was calculated using the equation described in Section 2.2.

2.4. Superoxide Anion Radical Scavenging Assay. The scavenging activity against the superoxide anion radical was measured based on the reduction of nitro blue tetrazolium (NBT) by superoxide generated in an NADH/phenazine methosulfate (PMS) system.[27] Reagents were prepared in 20 mM potassium phosphate buffer (pH 7.4) as follows: 78 μM NBT, 468 μM NADH, and serially diluted samples of Rutin, αG-Rutin, and ascorbic acid as a control, at final concentrations ranging from 1.56 to 400 μM. Compound stock solutions (12 mM) were prepared in DMSO. For each reaction, 50 μL of NBT, 50 μL of NADH, and 50 μL of the test solution were mixed in a 96-well clear microplate. For control wells, 50 μL of DMSO was added instead of the test solution. Due to the intrinsic yellow color of Rutin and αG-Rutin, sample blanks were prepared by combining 50 μL of the test solution with 120 μL of buffer (excluding other assay reagents) to correct for background absorbance. The reaction was initiated by adding 20 μL of 60 μM PMS (in 20 mM potassium phosphate buffer, pH 7.4). After 5 min of incubation at 37 °C, the absorbance was measured at 560 nm using a SpectraMax M2e microplate reader (Molecular Devices). Radical scavenging activity was calculated using the equation described in Section 2.2.

2.5. Deoxyribose Assay. Hydroxyl radical scavenging activity was determined using a deoxyribose assay with minor modifications.[28] A 1 mL reaction mixture was prepared containing 2.8 mM deoxyribose, 25 μM $FeCl_3$, and 100 μM EDTA in 20 mM potassium phosphate buffer (pH 7.4). $FeCl_3$ and EDTA were premixed before adding deoxyribose to initiate Fenton-like reaction conditions. To each reaction tube, 12 μL of compound solution (or 12 μL of phosphate buffer for control), 10 μL of the reaction mixture, and 8 μL of 8.4 mM H_2O_2 were added. The reaction was initiated by adding 6 μL of 600 μM ascorbic acid, resulting in final concentrations of antioxidant compounds, Rutin, αG-Rutin, and BHT (2,6-Di*tert*-butyl-p-cresol) as a control, ranging from 1.56 to 400 μM. The mixtures were incubated at 37 °C for 1 h. Following incubation, 30 μL of 1% (w/v) thiobarbituric acid (TBA) and 30 μL of 2.8% (w/v) trichloroacetic acid (TCA) were added. The samples were then heated at 100 °C for 20 min, cooled to

https://doi.org/10.1021/acsnutrsci.5c00012
ACS Nutr. Sci. XXXX, XXX, XXX−XXX

room temperature, and 96 μL of 1-butanol was added. After vortexing and centrifugation, the upper organic phase containing the colored product was transferred to a 96-well microplate. Absorbance was measured at 532 nm using a SpectraMax M2e microplate reader (Molecular Devices). Radical scavenging activity was calculated as described in Section 2.2.

2.6. Cell Culture. Normal human fibroblast TIG-1−20 cells (JCRB0501) were obtained from JCRB Cell Bank (Tokyo, Japan). Cells were cultured in Dulbecco's Modified Eagle Medium (DMEM), high glucose, supplemented with GlutaMAX and pyruvate (Thermo Fisher Scientific, Waltham, MA, USA), 10% fetal bovine serum (Sigma-Aldrich, St. Louis, MO, USA), and penicillin−streptomycin mixed solution (Nacalai Tesque, Kyoto, Japan). Cells were maintained at 37 °C in a humidified incubator with 5% CO_2. Subculturing was performed upon reaching 70−80% confluency using 0.25% trypsin-EDTA (Nacalai Tesque, Kyoto, Japan).

2.7. Cytotoxicity Assay. The cytotoxicity of the compounds was evaluated using a colorimetric assay with Cell Count Reagent SF (Nacalai Tesque, Kyoto, Japan), according to the manufacturer's instructions. Briefly, TIG-1 cells were seeded in 96-well clear microplates at a density of 5.0×10^3 cells per well in 100 μL of culture medium and incubated for 24 h. Test solutions (10 μL) were then added to each well to achieve final concentrations ranging from 5 to 100 μg/mL, with a final DMSO concentration of 0.5% in all wells. Following a 48 h incubation, 10 μL of Cell Count Reagent SF was added to each well, and the plates were incubated for an additional 1 h. Absorbance at 450 nm was measured using a SpectraMax M2e microplate reader (Molecular Devices) to assess cell viability.

2.8. Intracellular ROS Quantification by DCFDA. Intracellular ROS (Reactive Oxygen Species) levels were quantified using a DCFDA assay with slight modifications.[29] TIG-1 cells were seeded in black 96-well microplates at a density of 1.0×10^4 cells per well in 100 μL of culture medium. After 24 h, the medium was replaced with fresh medium containing Rutin or αG-Rutin (final DMSO concentration of 0.5% in all wells). Following a 24 h pretreatment, the media were removed and replaced with 20 μM DCFDA in FluoroBrite DMEM (Thermo Fisher Scientific), containing the same concentration of Rutin or αG-Rutin used during the pretreatment. Cells were incubated with DCFDA for 30 min, after which the dye solution was removed, and the wells were washed with Dulbecco's phosphate-buffered saline (D-PBS). Subsequently, 50 μM hydrogen peroxide (H_2O_2) in FluoroBrite DMEM was added, and cells were incubated for an additional 1 h. Fluorescence was then measured at an excitation/emission wavelength of 485/535 nm using a SpectraMax M2e microplate reader (Molecular Devices).

2.9. Measurement of 8-oxoG by Immunostaining. The levels of 8-oxoguanine (8-oxoG) were quantified by immunostaining using an anti-8-hydroxyguanosine DNA/RNA Oxidative Damage (QED Bioscience, San Diego, CA, USA). TIG-1 cells were treated with 150 μM αG-Rutin for 24 h, followed by exposure to 50 μM hydrogen peroxide (H_2O_2) for 1 h. Cells were then fixed with 3.7% formaldehyde for 10 min, permeabilized with 0.1% Triton X-100 for 15 min, and blocked with 2% bovine serum albumin (BSA) for 1 h at room temperature. After blocking, cells were incubated with the primary anti-8-oxoG antibody for 16 h at room temperature. Following thorough washing, cells were incubated with Alexa Fluor 647-conjugated goat polyclonal antibody to mouse IgG (Abcam) for 1 h. Hoechst 33342 was used for nuclear counterstaining to facilitate cell counting. Fluorescence imaging was performed using an FLUOVIEW FV1200 confocal fluorescence microscope (OLYMPUS). Image analysis was performed using Fiji (ImageJ). The total fluorescence intensity of Alexa Fluor 647 in each image was quantified and normalized to the number of nuclei stained with Hoechst 33342, enabling per-cell quantification of 8-oxoG levels.

2.10. Telomere Shortening over Replicative Aging. The experimental procedure is shown in Figure 4A. To induce telomere shortening via replicative aging, TIG-1 cells were continuously cultured for 10 passages (from passage number 9 to 19; population doubling level [PDL] approximately 30−60) over 6 weeks in the presence or absence of 30 μM αG-Rutin. Genomic DNA (gDNA) was extracted from early passage cells (passage number 9) before treatment. After 10 passages, gDNA was extracted from all the experimental groups. DNA extraction was performed using the DNeasy Blood and Tissue Kit (QIAGEN, Venlo, Netherlands) according to the manufacturer's instructions. Telomere length was determined by a quantitative PCR (qPCR)-based method as previously described method.[30,31]

2.11. Telomere Shortening under Chronic Oxidative Stress Condition. To induce telomere shortening via oxidative damage, TIG-1 cells were cultured for 2 weeks in growth medium supplemented with 10 μM H_2O_2. Telomere length was compared in the presence of 30 and 150 μM αG-Rutin, as well as under αG-Rutin-free conditions. After 2 weeks, gDNA was extracted from all experimental groups, and telomere length was determined using quantitative PCR.

2.12. Evaluation of IL-6 Expression under Oxidative Stress Condition. To increase the expression level of IL-6 via oxidative damage, TIG-1 cells were cultured for 2 weeks in growth medium supplemented with 10 μM H_2O_2 or exposed to 250 μM H_2O_2 for 12 h following a previously reported method with some modifications.[32] Comparisons of IL-6 expression levels were performed in the presence of 30 and 150 μM αG-Rutin, as well as under αG-Rutin-free conditions. After H_2O_2 treatment, total RNA was extracted from all samples using FastGene RNA Basic Kit (Nippon Genetics, Tokyo, Japan), reverse-transcribed using ReverTra Ace qPCR RT Master Mix with gDNA Remover (TOYOBO, Osaka, Japan), and the expression of beta-actin (ACTB) and interleukin-6 (IL-6) mRNAs was quantified by quantitative PCR. Primer sequences are shown in Table S2. Relative expression was calculated using the $\Delta\Delta Ct$ method, with ACTB as the endogenous control.

2.13. Evaluation of SA-βGal Expression under Oxidative Stress Condition. To induce oxidative stress-mediated premature senescence, TIG-1 cells were pretreated with αG-Rutin (30 μM or 150 μM) for 2 h. After pretreatment, cells were exposed to 100 μM H_2O_2 for 2 h and allowed to recover in fresh medium for 48 h following a previously reported method with some modifications.[33] After cellular recovery, cells were treated with 1 μM SPiDER-βGal (Dojindo, Kumamoto, Japan) for 30 min in a CO_2 incubator, following the manufacturer's instructions. Fluorescence was measured at excitation/emission wavelengths of 500/550 nm using a SpectraMax M2e microplate reader (Molecular Devices).

2.14. Statistical Analysis. All data are presented as mean ± standard deviation (SD). Statistical significance was assessed using one-way ANOVA, followed by Dunnett's multiple

https://doi.org/10.1021/acsnutrsci.5c00012
ACS Nutr. Sci. XXXX, XXX, XXX−XXX

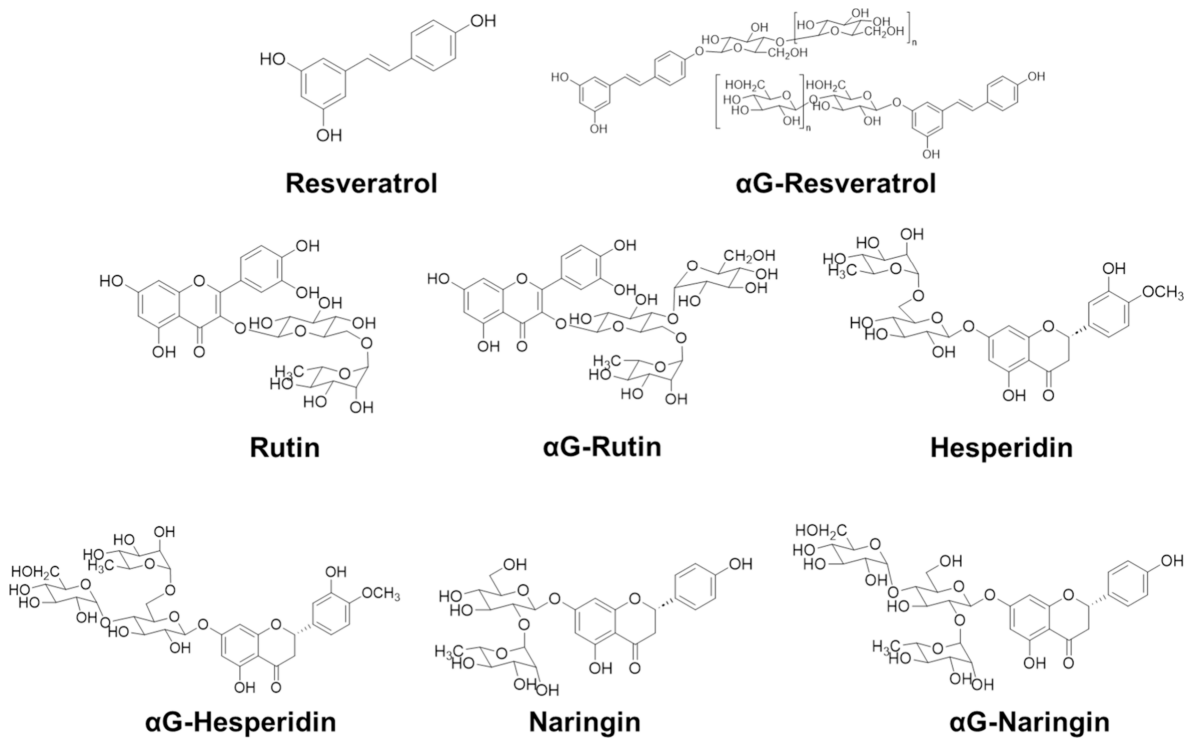

Figure 1. Chemical structures of polyphenols and their transglycosylated derivatives.

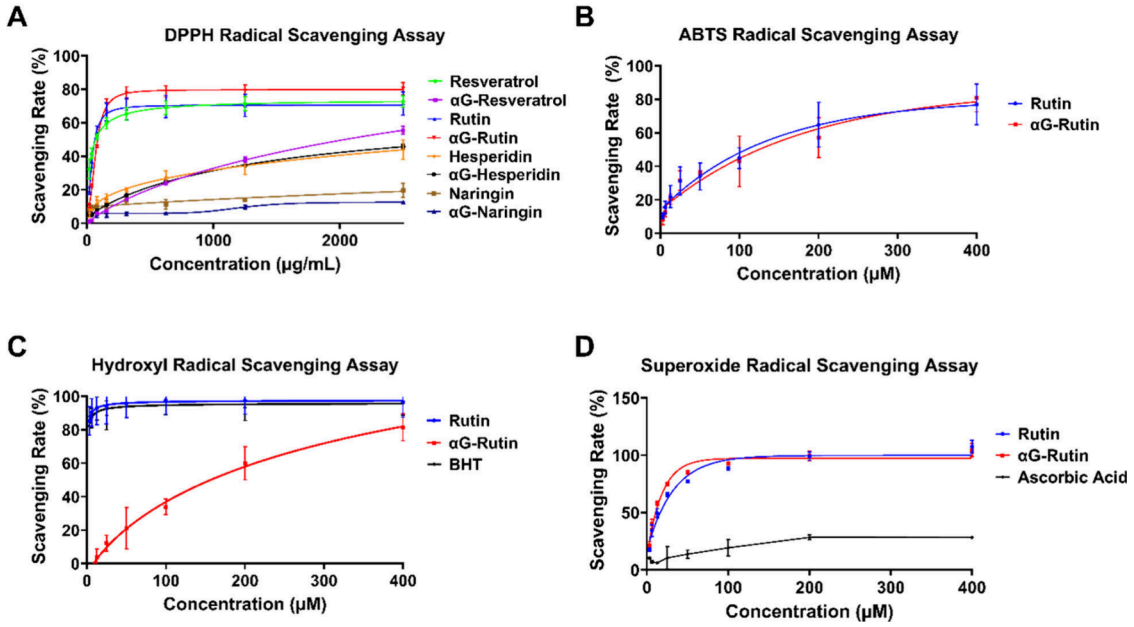

Figure 2. (A) DPPH radical scavenging activity of respective polyphenols and their transglycosylated derivatives; data is presented as mean ± SD (B) ABTS radical scavenging activity of Rutin and αG-Rutin; data is presented as mean ± SD (C) Hydroxyl radical scavenging activity of Rutin, αG-Rutin, and BHT as a control measured using the deoxyribose assay; data is presented as mean ± SD (D) Superoxide anion scavenging activity of Rutin, αG-Rutin, and ascorbic acid as a control; data is presented as mean ± SD.

comparisons test, as appropriate. Statistical p-value less than 0.05 ($p < 0.05$) was considered statistically significant. All statistical analyses were performed using GraphPad Prism version 10.4.1 (GraphPad Software, San Diego, CA, USA).

3. RESULTS

3.1. αG-Rutin Exhibits Stronger Antioxidant Activity. We initially aimed to evaluate the antioxidant capacity of the polyphenols (Resveratrol, Hesperidin, Naringin, and Rutin) in comparison to their glycosylated derivatives (Figure 1), which are known to have improved water solubility and bioavailability.[34] To this end, we performed the DPPH radical scavenging assay, a widely used method to assess the electron-donating ability of antioxidant compounds.[35] Among the tested polyphenols, Resveratrol and Rutin exhibited a pronounced capacity to reduce the stable purple-colored

https://doi.org/10.1021/acsnutrsci.5c00012
ACS Nutr. Sci. XXXX, XXX, XXX−XXX

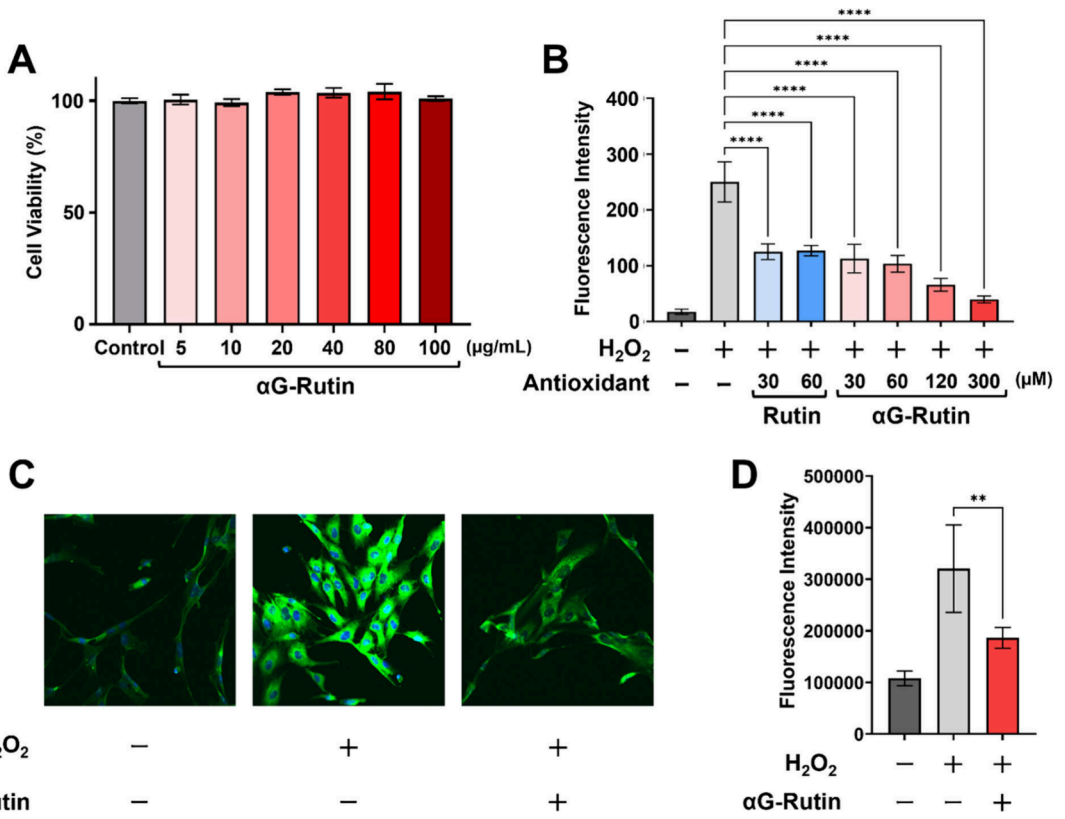

Figure 3. (A) Cytotoxicity of αG-Rutin in TIG-1 cells. Cells were treated with 5−100 μg/mL of αG-Rutin for 48 h, and cell viability was assessed; data is presented as mean ± SD (B) Intracellular ROS levels were measured using the DCFDA assay. TIG-1 cells were treated with Rutin or αG-Rutin for 24 h, followed by incubation with 20 μM DCFDA for 30 min. Cells were then exposed to 50 μM hydrogen peroxide for 1 h. Fluorescence was measured using a microplate reader (Ex/Em = 485/535 nm) (****$p < 0.0001$; mean ± SD). (C) 8-oxoG immunofluorescence staining to assess oxidative DNA damage. Cells were treated with αG-Rutin for 24 h, followed by 1 h exposure to 50 μM hydrogen peroxide. Blue indicates nuclei (Hoechst); green indicates 8-oxoG. Images were acquired using confocal fluorescence microscopy. (D) Quantification of 8-oxoG per cell. The fluorescence intensity of Alexa Fluor 647 (8-oxoG) was normalized to the number of Hoechst-stained nuclei (n = 185−221 cells). (**$p < 0.01$; mean ± SD).

DPPH radical to yellow-colored diphenylpicrylhydrazine, indicative of antioxidant activity. Notably, among the glycosylated derivatives, only αG-Rutin demonstrated substantial radical-scavenging activity, comparable to that of Rutin (Figure 2A, Table S1). The half-maximal inhibitory concentration (IC_{50}) was determined to be 77.48 μg/mL for Rutin and 102.24 μg/mL for αG-Rutin. In contrast, the antioxidant capacity of αG-Resveratrol decreased. This decrease is likely attributable to the conjugation of the sugar moiety to the phenolic hydroxyl group of resveratrol, which is crucial for neutralizing free radicals.

Based on the DPPH assay results, αG-Rutin was selected for further analysis because of its strong antioxidant activity. The antioxidant potential was further assessed using the ABTS radical assay, which is known for its broad sensitivity.[36] Consistent with the DPPH radical assay findings, both Rutin and αG-Rutin demonstrated strong ABTS radical-scavenging activity (Figure 2B). The IC_{50} values for Rutin and αG-Rutin were determined to be 126.8 μM and 149.5 μM, respectively, while the positive control, Trolox, exhibited an IC_{50} of 12.46 μM. Hydroxyl radicals are highly potent oxidants that react with virtually all biomolecules in living cells. The capacities of Rutin and αG-Rutin to scavenge these radicals and prevent deoxyribose substrate degradation were evaluated. As shown in Figure 2C, both the positive control, BHT, and Rutin displayed strong antioxidant activity. The glycosylated derivative, αG-Rutin, also demonstrated hydroxyl radical scavenging activity, albeit at a reduced level compared to that of Rutin. This diminished activity can be attributed to the enlarged glycosyl moiety, which increases steric hindrance and decreases molecular planarity, thereby interfering with hydrogen-atom donation and resonance stabilization of the resulting phenoxyl radical, consistent with previous reports on glycosylated quercetin.[37] Finally, the antioxidant activity against superoxide radicals, which act as precursors to other ROS and can be particularly damaging to cells, was evaluated. Under our assay conditions, both αG-Rutin and Rutin exhibited substantially stronger superoxide-radical-scavenging activity than ascorbic acid, a widely used standard reference compound.[38−40] While Rutin is recognized as a potent superoxide anion radical scavenger,[27,41,42] its derivative αG-Rutin also possesses a comparable activity levels.

3.2. αG-Rutin demonstrated strong intracellular antioxidant activity and DNA protection effects. Based on the initial *in vitro* assessment of antioxidant activity, αG-Rutin was identified as the most promising candidate. To further evaluate its efficacy at the cellular level, we selected TIG-1 cells, a well-established model for studying telomere shortening and cellular senescence. We first assessed the cytotoxicity of αG-Rutin at various concentrations using the WST-8 assay. As shown in Figure 3A, treatment with αG-Rutin at different concentrations ranging from 5 to 100 μg/mL for 48

https://doi.org/10.1021/acsnutrsci.5c00012
ACS Nutr. Sci. XXXX, XXX, XXX−XXX

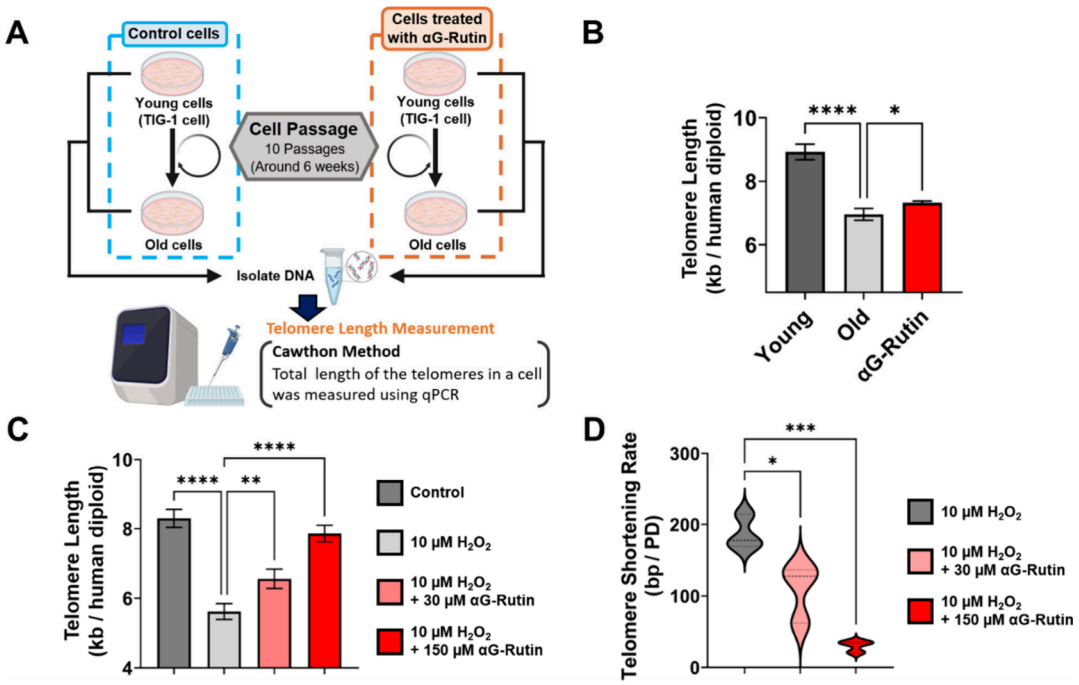

Figure 4. (A) Schematic representation of the method used to evaluate telomere shortening during long-term cell passage; created with BioRender.com. (B) Assessment of telomere length by real-time qPCR following long-term culture with or without αG-Rutin; "Young" represents telomere length of TIG-1 cells before 10 passages; "Old" represents telomere length after 10 passages without αG-Rutin; "αG-Rutin" indicates telomere length after 10 passages in the presence of 30 μM αG-Rutin (****$p < 0.0001$, *$p < 0.05$; mean ± SD). (C) Assessment of telomere length (TL) by real-time qPCR following two-week cell culture under chronic oxidative stress induced by 10 μM H_2O_2 with or without αG-Rutin; "Control" represents telomere length of TIG-1 cells before two-week treatment (****$p < 0.0001$, **$p < 0.01$; mean ± SD). (D) Telomere shortening rate (bp/PD) under chronic oxidative condition with or without αG-Rutin; data is presented by violin plot showing the kernel density of the data (***$p < 0.001$, *$p < 0.05$).

h showed no significant cell death. Subsequently, we performed an intracellular ROS quantification assay using the DCFDA probe (Figure 3B). Intracellular ROS was induced using H_2O_2, which led to an increase in DCFDA fluorescence intensity in TIG-1 cells, indicating intracellular ROS induction. Pretreatment with Rutin reduced intracellular ROS levels at 30 and 60 μM. While αG-Rutin exhibited effects similar to those of Rutin at lower concentrations, at higher concentrations, where αG-Rutin remained soluble unlike Rutin, it demonstrated markedly greater intracellular ROS-scavenging ability. This highlights its potential as a more effective antioxidant under physiologically relevant conditions for mitigating oxidative stress within the cellular environment.

To further investigate the antioxidant potential of αG-Rutin, we examined its capacity to prevent oxidative DNA/RNA damage, focusing on the formation of 8-oxoG. 8-oxoG is the most abundant oxidative lesion arising from guanine, which is particularly vulnerable to ROS-induced damage due to its low redox potential. To evaluate the 8-oxoG levels, we performed immunofluorescence staining using an anti-8-oxoG antibody. TIG-1 cells were treated with or without αG-Rutin, followed by exposure to H_2O_2 to induce oxidative stress. As shown in Figure 3C and 3D, treatment with H_2O_2 alone resulted in a marked increase in 8-oxoG signals, indicating substantial oxidative DNA/RNA damage in the cells. In contrast, cells pretreated with αG-Rutin exhibited a significant reduction in 8-oxoG accumulation. Quantification of fluorescence intensity from over 180 cells demonstrated an approximately 1.75-fold reduction in 8-oxoG levels compared to H_2O_2 treatment. These results are consistent with the in vitro hydroxyl and superoxide anion radical scavenging activities of αG-Rutin. Since hydroxyl radicals cause both deoxyribose degradation and oxidative DNA lesions like 8-oxoG, and superoxide anion radicals are the most frequently produced ROS in cells as well as precursors to hydroxyl radicals, the ability of αG-Rutin to neutralize these radicals supports its protective role against ROS-induced DNA damage.

3.3. Suppression of telomere attrition and cellular senescence by αG-Rutin. Given that oxidative stress is implicated in numerous human disease etiologies and premature aging by accelerating telomere attrition, we sought to evaluate whether αG-Rutin can prevent telomere shortening.[12] To this end, we modeled replicative aging by culturing TIG-1 cells through serial passages with and without αG-Rutin treatment over 10 passages, as outlined in Figure 4A. Telomere length was measured using the Cawthon method, which determines relative telomere length based on the telomere repeat copy number normalized to a single-copy reference gene. As shown in Figure 4B, replicative aging of TIG-1 cells over 10 passages resulted in a substantial reduction in telomere length up to 2.0 ± 0.31 kb compared to young-passaged cells. In TIG-1 cells, exposure to 30 μM αG-Rutin resulted in up to an 18.6 ± 10.3% suppression of telomere shortening compared with untreated aged controls. To enable direct comparison across compounds at an equivalent concentration, we adopted a lower concentration as the test condition, constrained by the limited aqueous solubility of αG-Resveratrol, which was assessed in parallel. Under these conditions, the other transglycosylated conjugates (αG-Resveratrol, αG-Hesperidin, and αG-Naringin) did not exhibit significant suppression of telomere shortening, with telomere lengths remaining indistinguishable from those of the untreated control (Figure S1).

https://doi.org/10.1021/acsnutrsci.5c00012
ACS Nutr. Sci. XXXX, XXX, XXX−XXX

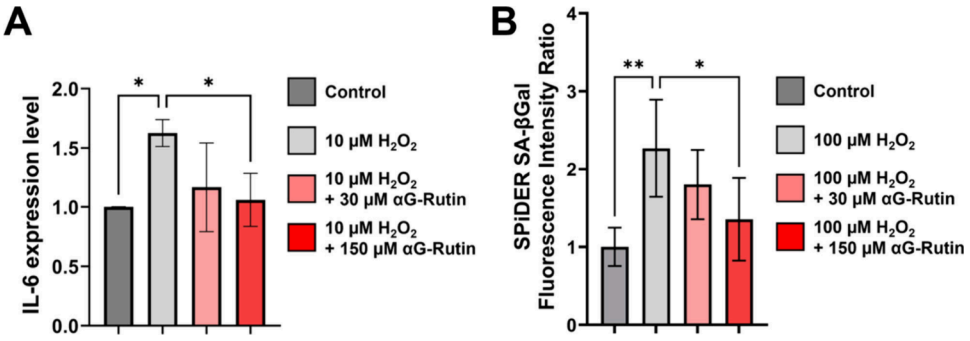

Figure 5. (A) Evaluation of IL-6 expression levels by RT-qPCR following two-week under chronic oxidative stress induced by 10 μM H_2O_2 with or without αG-Rutin; "Control" represents telomere length of TIG-1 cells before two-week treatment (*$p < 0.05$; mean ± SD). (B) TIG-1 cells were treated for 2 h with 100 μM H_2O_2 in the presence or absence of αG-Rutin (30 or 150 μM), then allowed to recover for 48 h. SA β-Gal activity was quantified by fluorescence and normalized to the untreated control. (**$p < 0.01$, *$p < 0.05$; mean ± SD).

This finding further underscores the specificity of αG-Rutin in mediating telomere attrition suppression.

To determine whether αG-Rutin can suppress telomere attrition under chronic oxidative stress conditions, we employed a long-term H_2O_2 exposure model. Two-week culture with 10 μM H_2O_2 resulted in a significant decrease in telomere length up to 2.68 ± 0.34 kb (Figure 4C). In contrast, cotreatment with αG-Rutin (30 or 150 μM) attenuated telomere shortening in a concentration-dependent manner. From the regression slopes shown in Figure 4D, the shortening rate under oxidative stress alone was ∼ 187 bp per PD, consistent with prior reports of H_2O_2-induced telomere erosion.[13] Treatment with 30 μM αG-Rutin reduced the estimated telomere shortening rate to ∼ 109 bp per PD; notably, a further decrease to ∼ 30 bp per PD was observed at 150 μM, a level comparable to replication-driven shortening,[43,44] thereby indicating strong suppression of oxidative telomere damage.

Because telomere attrition is an established trigger of senescence-associated inflammation,[45] we next examined whether αG-Rutin influences IL-6 expression under chronic oxidative stress. Quantification of IL-6 expression using RNA extracted from cells cultured for 2 weeks with 10 μM H_2O_2, where telomere shortening had been verified in Figure 4C, revealed an approximately 1.6-fold upregulation (Figure 5A). Consistent with the results of telomere length, this pro-inflammatory response was also significantly suppressed by αG-Rutin. This finding suggests that αG-Rutin may suppress the emergence of downstream senescence-associated phenotypes by preventing telomere shortening.

Finally, to test whether αG-Rutin also protects against senescence induced independently of telomere shortening, we used an acute oxidative stress model. We first quantified cellular senescence using a sensitive fluorescent probe (SPiDER-βGal) for measuring senescence-associated β-galactosidase (SA-βGal) activity. Acute 100 μM H_2O_2 exposure induced a significant 2-fold increase in SA-βGal activity (**$p <$ 0.01), confirming the induction of senescence (Figure 5B). This effect was dose-dependently attenuated by cotreatment with αG-Rutin; notably, the 150 μM concentration completely abrogated the H_2O_2-induced signal, restoring the activity to control levels. We also quantified IL-6 expression levels because it is known to be overexpressed under strong oxidative conditions, which resulted in αG-Rutin suppressing IL-6 expression, consistent with the result of SA-βGal (Figure S2). Taken together, these data demonstrate that the capacity of αG-Rutin to scavenge intracellular ROS and suppress oxidative damage not only prevents telomere attrition but also suppresses pro-inflammatory secretory function and other molecular markers of senescence.

In summary, our findings indicate that αG-Rutin exhibits significant antioxidant activity both *in vitro* and *in cellulo* without inducing any cytotoxicity. The improved solubility of αG-Rutin compared to that of Rutin enhances its ability to scavenge intracellular ROS and mitigate oxidative DNA damage, as evidenced by reduced 8-oxoG levels. Furthermore, αG-Rutin treatment preserved telomere length under chronic oxidative conditions and replicative aging and prevented the onset of senescence. These results suggest that αG-Rutin holds promise as a therapeutic candidate for addressing oxidative stress-induced and age-related telomere attrition and senescence. Further research is necessary to validate its efficacy *in vivo* and explore its potential as a functional ingredient or nutraceutical.

4. DISCUSSION

For decades, strategies to extend health span and prolong longevity have been the focus of research. Among them, small molecules and antioxidant compounds that slow down telomere shortening, a process driven by cumulative oxidative stress and diminished telomerase activity, are promising. In this regard, several natural products, including TA-65,[46] cycloastragenol,[47] ergothioneine,[48] and caffeine,[49] have been reported to counteract telomere shortening. Furthermore, several clinical cohort studies also demonstrate that a diet rich in polyphenols slows down telomere shortening, which might play a role in increased lifespan.[50,51] However, the effect of antioxidant polyphenols is hindered by their low solubility and bioavailability, limiting their practical application.[52]

In the current study, we investigated the *in vitro* antioxidant activities of transglycosylated polyphenols with enhanced water solubility and identified αG-Rutin with enhanced scavenging activity (Figure 2). We investigated the effects of αG-Rutin on cell viability, intracellular ROS scavenging, oxidative DNA damage, and telomere protection in fibroblasts (Figures 3 and 4). Cell viability assay demonstrated no cytotoxicity at various concentrations, indicating its safe profile. Subsequent *in cellulo* results also revealed that αG-Rutin mitigated intracellular ROS levels compared to Rutin at higher concentrations, where it remained soluble.

Elevated ROS levels also contribute to oxidative DNA/RNA damage, especially guanine damage, due to its low redox

https://doi.org/10.1021/acsnutrsci.5c00012
ACS Nutr. Sci. XXXX, XXX, XXX−XXX

potential, often resulting in the formation of mutagenic lesions such as 8-oxoG. In our study, treatment with αG-Rutin significantly reduced 8-oxoG levels as evidenced by immunostaining. While it remains uncertain whether αG-Rutin is directly taken up into the nucleus, the overall decrease in intracellular ROS levels (Figure 3B) suggests that passively diffused αG-Rutin within the cell contributes to this protection by scavenging ROS throughout the cell. Our observation was also consistent with a previous study in which αG-Rutin treatment increased the viability of induced pluripotent stem cells (iPSCs) by maintaining genomic stability.[53] Using a quantitative PCR-based approach, we observed a reduction in telomere attrition in αG-Rutin-treated cells compared to the untreated control in both the replicative aging and chronic oxidative stress models. Notably, in the chronic oxidative stress model, telomere shortening was suppressed by αG-Rutin in a dose-dependent manner. This protective effect can be attributed to enhanced protection from intracellular oxidative stress and a reduced incidence of guanine oxidation in the telomere region, which is consistent with our *in vitro* studies and also a previous study using pulse-radiolysis.[54] Furthermore, IL-6 expression, an inflammatory cytokine downstream of telomere shortening and cellular senescence, decreased in a concentration-dependent manner upon αG-Rutin treatment. These findings suggest that αG-Rutin not only suppresses telomere shortening under chronic oxidative conditions but may also attenuate associated cellular senescence. Previous studies have also reported that excessive intracellular oxidative damage or the formation of telomeric 8-oxoG alone drives rapid premature senescence, even in the absence of telomere shortening.[14,15] Our findings further demonstrate that αG-Rutin not only reduces 8-oxoG levels and preserves telomere length but also suppresses key senescence markers, including SA-β-gal activity and IL-6 expression, under acute oxidative stress conditions (Figure 5B and S2). Taken together, these results suggest that αG-Rutin may delay cellular senescence through dual mechanisms: by preventing telomere shortening via ROS scavenging and by blocking oxidative damage-induced senescence signaling independent of telomere length changes. This multifaceted effect supports further investigation of αG-Rutin as a potential approach for telomere protection and mitigation of premature cellular aging.

Our study demonstrates the promising effect of αG-Rutin in mitigating telomere attrition in our replicative aging model; however, this *in cellulo* system cannot fully recapitulate the complex aging process observed *in vivo*. While our fibroblast model yields valuable insights, further investigations employing *in vivo* models are necessary to substantiate the efficacy of αG-Rutin, which is currently in progress. While animal studies indicate superior absorption of αG-Rutin to Rutin[34] and a regimen of 200 or 400 mg/day for 8 weeks has been reported to be beneficial,[23,55] human bioavailability and exposure remain uncharacterized, which constrains translational interpretation. Moreover, the 150 μM concentration used under oxidative stress conditions was selected for mechanistic interrogation rather than reflecting physiologically achievable levels. Although effects were observed at 30 μM, establishing the oral dose required to achieve efficacious intracellular concentrations *in vivo* is critical for functional food applications. Future pharmacokinetic studies are needed to bridge the gap between *in vitro* efficacy and practical human exposures.

In conclusion, our study demonstrates that αG-Rutin, a glycosylated derivative of Rutin, exhibits potent antioxidant activity both *in vitro* and *in cellulo*. Notably, αG-Rutin showed enhanced intracellular ROS scavenging compared to Rutin, which remained insoluble at higher concentrations. Furthermore, αG-Rutin conferred a protective effect against oxidative DNA damage, thereby reducing the levels of 8-oxoG. Finally, treatment with αG-Rutin in TIG-1 cells under chronic oxidative conditions and replicative aging attenuated telomere shortening and senescence, which can be attributed to enhanced ROS scavenging activity and reduced formation of 8-oxoG. Overall, αG-Rutin emerges as a promising antioxidant with therapeutic relevance in age-related pathologies linked to oxidative stress and telomere attrition.

■ ASSOCIATED CONTENT

Supporting Information

The Supporting Information is available free of charge at https://pubs.acs.org/doi/10.1021/acsnutrsci.5c00012.

Primer sequences of ACTB and IL-6, IC_{50} values (μg/mL) for the reduction of the DPPH radical, the telomere length measurement using Cawthon method after replicative aging, and IL-6 expression levels under acute oxidative stress (PDF)

■ AUTHOR INFORMATION

Corresponding Author

Hiroshi Sugiyama − *Department of Chemistry, Graduate School of Science, Kyoto University, Sakyo-Ku, Kyoto 606-8502, Japan; Institute for Integrated Cell-Material Sciences (WPI-iCeMS), Kyoto University, Sakyo-Ku, Kyoto 606-8501, Japan;* orcid.org/0000-0001-8923-5946; Email: sugiyama.hiroshi.3s@kyoto-u.ac.jp

Authors

Takumi Terada − *Department of Chemistry, Graduate School of Science, Kyoto University, Sakyo-Ku, Kyoto 606-8502, Japan*

Vinodh J Sahayasheela − *Department of Chemistry, Graduate School of Science, Kyoto University, Sakyo-Ku, Kyoto 606-8502, Japan; Institute for Integrated Cell-Material Sciences (WPI-iCeMS), Kyoto University, Sakyo-Ku, Kyoto 606-8501, Japan; Human Biology Microbiome Quantum Research Center (WPI-Bio2Q), Keio University, Tokyo 160-8582, Japan;* orcid.org/0000-0001-8231-3286

Ryohei Noizumi − *Department of Chemistry, Graduate School of Science, Kyoto University, Sakyo-Ku, Kyoto 606-8502, Japan*

Akihito Nakanishi − *Toyo Sugar Refining Company, Limited, Chuo-ku, Tokyo 103-0016, Japan*

Mahamadou Tandia − *Toyo Sugar Refining Company, Limited, Chuo-ku, Tokyo 103-0016, Japan*

Complete contact information is available at: https://pubs.acs.org/10.1021/acsnutrsci.5c00012

Author Contributions

V.J.S., M.T., A.N., and H.S. conceived the study. V.J.S. and T.T. designed the work. T.T., V.J.S., and R.N. performed research. V.J.S. and T.T. wrote the manuscript.

Notes

The authors declare no competing financial interest.

■ ACKNOWLEDGMENTS

This work was supported by funding from Toyo Sugar Refining Company, Limited. Graphical abstract and Figure 4A were created with BioRender.com.

■ ABBREVIATIONS

DCFDA	2′,7′-dichlorodihydrofluorescein diacetate
ROS	reactive oxygen species
PMS	phenazine methyl sulfate
NADH	nicotinamide adenine dinucleotide, reduced form
EDTA	ethylendiaminetetraacetic acid
DMSO	dimethyl sulfoxide
BHT	2,6-Di*tert*-butyl-*p*-cresol

■ REFERENCES

(1) López-Otín, C.; Blasco, M. A.; Partridge, L.; Serrano, M.; Kroemer, G. Hallmarks of Aging: An Expanding Universe. *Cell* **2023**, *186* (2), 243−278.
(2) Armanios, M.; Blackburn, E. H. The Telomere Syndromes. *Nat. Rev. Genet.* **2012**, *13* (10), 693−704.
(3) de Lange, T. Shelterin: The Protein Complex That Shapes and Safeguards Human Telomeres. *Genes Dev.* **2005**, *19* (18), 2100−2110.
(4) O'Sullivan, R. J.; Karlseder, J. Telomeres: Protecting Chromosomes against Genome Instability. *Nat. Rev. Mol. Cell Biol.* **2010**, *11* (3), 171−181.
(5) Whittemore, K.; Vera, E.; Martínez-Nevado, E.; Sanpera, C.; Blasco, M. A. Telomere Shortening Rate Predicts Species Life Span. *Proc. Natl. Acad. Sci. U. S. A.* **2019**, *116* (30), 15122−15127.
(6) Muñoz-Lorente, M. A.; Cano-Martin, A. C.; Blasco, M. A. Mice with Hyper-Long Telomeres Show Less Metabolic Aging and Longer Lifespans. *Nat. Commun.* **2019**, *10* (1), 4723.
(7) McHugh, D.; Gil, J. Senescence and Aging: Causes, Consequences, and Therapeutic Avenues. *J. Cell Biol.* **2018**, *217* (1), 65−77.
(8) Correia-Melo, C.; Hewitt, G.; Passos, J. F. Telomeres, Oxidative Stress and Inflammatory Factors: Partners in Cellular Senescence? *Longev. Healthspan* **2014**, *3* (1), 1.
(9) von Zglinicki, T. Oxidative Stress Shortens Telomeres. *Trends Biochem. Sci.* **2002**, *27* (7), 339−344.
(10) Jacome Burbano, M. S.; Cherfils-Vicini, J.; Gilson, E. Neutrophils: Mediating TelOxidation and Senescence. *EMBO J.* **2021**, *40* (9), No. e108164.
(11) Rhee, D. B.; Ghosh, A.; Lu, J.; Bohr, V. A.; Liu, Y. Factors That Influence Telomeric Oxidative Base Damage and Repair by DNA Glycosylase OGG1. *DNA Repair (Amst.)* **2011**, *10* (1), 34−44.
(12) Rossiello, F.; Jurk, D.; Passos, J. F.; d'Adda di Fagagna, F. Telomere Dysfunction in Ageing and Age-Related Diseases. *Nat. Cell Biol.* **2022**, *24* (2), 135−147.
(13) von Zglinicki, T.; Pilger, R.; Sitte, N. Accumulation of Single-Strand Breaks Is the Major Cause of Telomere Shortening in Human Fibroblasts. *Free Radic. Biol. Med.* **2000**, *28* (1), 64−74.
(14) Gorbunova, V.; Seluanov, A.; Pereira-Smith, O. M. Expression of Human Telomerase (HTERT) Does Not Prevent Stress-Induced Senescence in Normal Human Fibroblasts but Protects the Cells from Stress-Induced Apoptosis and Necrosis. *J. Biol. Chem.* **2002**, *277* (41), 38540−38549.
(15) Barnes, R. P.; de Rosa, M.; Thosar, S. A.; Detwiler, A. C.; Roginskaya, V.; Van Houten, B.; Bruchez, M. P.; Stewart-Ornstein, J.; Opresko, P. L. Telomeric 8-Oxo-Guanine Drives Rapid Premature Senescence in the Absence of Telomere Shortening. *Nat. Struct. Mol. Biol.* **2022**, *29* (7), 639−652.
(16) Schellnegger, M.; Hofmann, E.; Carnieletto, M.; Kamolz, L.-P. Unlocking Longevity: The Role of Telomeres and Its Targeting Interventions. *Front. Aging* **2024**, *5*, No. 1339317.
(17) Panche, A. N.; Diwan, A. D.; Chandra, S. R. Flavonoids: An Overview. *J. Nutr. Sci.* **2016**, *5* (e47), No. e47.
(18) Chebil, L.; Humeau, C.; Anthoni, J.; Dehez, F.; Engasser, J.-M.; Ghoul, M. Solubility of Flavonoids in Organic Solvents. *J. Chem. Eng. Data* **2007**, *52* (5), 1552−1556.
(19) Khodzhaieva, R. S.; Gladkov, E. S.; Kyrychenko, A.; Roshal, A. D. Progress and Achievements in Glycosylation of Flavonoids. *Front. Chem.* **2021**, *9*, No. 637994.
(20) Suzuki, Y.; Suzuki, K. Enzymatic Formation of 4G-α-d-Glucopyranosyl-Rutin. *Agric. Biol. Chem.* **1991**, *55* (1), 181−187.
(21) Muvhulawa, N.; Dludla, P. V.; Ziqubu, K.; Mthembu, S. X. H.; Mthiyane, F.; Nkambule, B. B.; Mazibuko-Mbeje, S. E. Rutin Ameliorates Inflammation and Improves Metabolic Function: A Comprehensive Analysis of Scientific Literature. *Pharmacol. Res.* **2022**, *178*, No. 106163.
(22) Choi, S. S.; Park, H. R.; Lee, K. A. A Comparative Study of Rutin and Rutin Glycoside: Antioxidant Activity, Anti-Inflammatory Effect, Effect on Platelet Aggregation and Blood Coagulation. *Antioxidants* **2021**, *10* (11), 1696.
(23) Hashizume, Y.; Tandia, M. Monoglucosyl Rutin, a Flavonoid Glycoside, Improves Low-Density Lipoprotein-Cholesterol Levels in Healthy Adults: A Randomized Controlled Trial. *Funct. Foods Health Dis.* **2024**, *14* (6), 222−235.
(24) Nishikawa, S.; Hyodo, T.; Nagao, T.; Nakanishi, A.; Tandia, M.; Tsuda, T. A. -Monoglucosyl Hesperidin but Not Hesperidin Induces Brown-like Adipocyte Formation and Suppresses White Adipose Tissue Accumulation in Mice. *J. Agric. Food Chem.* **2019**, *67* (7), 1948−1954.
(25) Uchiyama, H.; Minoura, K.; Yamada, E.; Ando, K.; Yamauchi, R.; Nakanishi, A.; Tandia, M.; Kadota, K.; Tozuka, Y. Solubilization Mechanism of α-Glycosylated Naringin Based on Self-Assembled Nanostructures and Its Application to Skin Formulation. *Eur. J. Pharm. Biopharm.* **2024**, *200*, No. 114316.
(26) Nenadis, N.; Wang, L.-F.; Tsimidou, M.; Zhang, H.-Y. Estimation of Scavenging Activity of Phenolic Compounds Using the ABTS(*+) Assay. *J. Agric. Food Chem.* **2004**, *52* (15), 4669−4674.
(27) Yang, J.; Guo, J.; Yuan, J. In Vitro Antioxidant Properties of Rutin. *Lebenson. Wiss. Technol.* **2008**, *41* (6), 1060−1066.
(28) Aruoma, O. I. [5] Deoxyribose Assay for Detecting Hydroxyl Radicals. *Methods in Enzymology*; Elsevier, 1994; pp 57−66.
(29) Ng, N. S.; Ooi, L. A Simple Microplate Assay for Reactive Oxygen Species Generation and Rapid Cellular Protein Normalization. *Bio Protoc.* **2021**, *11* (1), No. e3877.
(30) Cawthon, R. M. Telomere Measurement by Quantitative PCR. *Nucleic Acids Res.* **2002**, *30* (10), No. e47.
(31) O'Callaghan, N. J.; Fenech, M. A Quantitative PCR Method for Measuring Absolute Telomere Length. *Biol. Proced. Online* **2011**, *13* (1), 3.
(32) Wu, W.-C.; Hu, D.-N.; Gao, H.-X.; Chen, M.; Wang, D.; Rosen, R.; McCormick, S. A. Subtoxic Levels Hydrogen Peroxide-Induced Production of Interleukin-6 by Retinal Pigment Epithelial Cells. *Mol. Vis.* **2010**, *16*, 1864−1873.
(33) Cai, Y.; Zhou, H.; Zhu, Y.; Sun, Q.; Ji, Y.; Xue, A.; Wang, Y.; Chen, W.; Yu, X.; Wang, L.; Chen, H.; Li, C.; Luo, T.; Deng, H. Elimination of Senescent Cells by β-Galactosidase-Targeted Prodrug Attenuates Inflammation and Restores Physical Function in Aged Mice. *Cell Res.* **2020**, *30* (7), 574−589.
(34) Shimoi, K.; Yoshizumi, K.; Kido, T.; Usui, Y.; Yumoto, T. Absorption and Urinary Excretion of Quercetin, Rutin, and AlphaG-Rutin, a Water Soluble Flavonoid, in Rats. *J. Agric. Food Chem.* **2003**, *51* (9), 2785−2789.
(35) Nampoothiri, S. V.; Prathapan, A.; Cherian, O. L.; Raghu, K. G.; Venugopalan, V. V.; Sundaresan, A. In Vitro Antioxidant and Inhibitory Potential of Terminalia Bellerica and Emblica Officinalis Fruits against LDL Oxidation and Key Enzymes Linked to Type 2 Diabetes. *Food Chem. Toxicol.* **2011**, *49* (1), 125−131.
(36) Re, R.; Pellegrini, N.; Proteggente, A.; Pannala, A.; Yang, M.; Rice-Evans, C. Antioxidant Activity Applying an Improved ABTS Radical Cation Decolorization Assay. *Free Radic. Biol. Med.* **1999**, *26* (9−10), 1231−1237.

https://doi.org/10.1021/acsnutrsci.5c00012
ACS Nutr. Sci. XXXX, XXX, XXX−XXX

(37) Cai, W.; Chen, Y.; Xie, L.; Zhang, H.; Hou, C. Characterization and Density Functional Theory Study of the Antioxidant Activity of Quercetin and Its Sugar-Containing Analogues. *Eur. Food Res. Technol.* **2014**, *238* (1), 121−128.
(38) Njus, D.; Kelley, P. M.; Tu, Y.-J.; Schlegel, H. B. Ascorbic Acid: The Chemistry Underlying Its Antioxidant Properties. *Free Radic. Biol. Med.* **2020**, *159*, 37−43.
(39) Govindan, P.; Muthukrishnan, S. Evaluation of Total Phenolic Content and Free Radical Scavenging Activity of Boerhavia Erecta. *J. Acute Med.* **2013**, *3* (3), 103−109.
(40) Jan, S.; Khan, M. R.; Rashid, U.; Bokhari, J. Assessment of Antioxidant Potential, Total Phenolics and Flavonoids of Different Solvent Fractions of Monotheca Buxifolia Fruit. *Osong Public Health Res. Perspect.* **2013**, *4* (5), 246−254.
(41) Sueishi, Y.; Hori, M.; Ishikawa, M.; Matsu-Ura, K.; Kamogawa, E.; Honda, Y.; Kita, M.; Ohara, K. Scavenging Rate Constants of Hydrophilic Antioxidants against Multiple Reactive Oxygen Species. *J. Clin. Biochem. Nutr.* **2014**, *54* (2), 67−74.
(42) Zhishen, J.; Mengcheng, T.; Jianming, W. The Determination of Flavonoid Contents in Mulberry and Their Scavenging Effects on Superoxide Radicals. *Food Chem.* **1999**, *64* (4), 555−559.
(43) Lorenz, M.; Saretzki, G.; Sitte, N.; Metzkow, S.; von Zglinicki, T. BJ Fibroblasts Display High Antioxidant Capacity and Slow Telomere Shortening Independent of HTERT Transfection. *Free Radic. Biol. Med.* **2001**, *31* (6), 824−831.
(44) Xu, J.; Yang, X. Will Cloned Animals Suffer Premature Aging–the Story at the End of Clones' Chromosomes. *Reprod. Biol. Endocrinol.* **2003**, *1* (1), 105.
(45) Rodier, F.; Campisi, J. Four faces of cellular senescence. *J. Cell Biol.* **2011**, *192* (4), 547−556.
(46) de Jesus, B.; Schneeberger, B.; Vera, K.; Tejera, E.; Harley, A.; Blasco, C. B. M. A. The Telomerase Activator TA-65 Elongates Short Telomeres and Increases Health Span of Adult/Old Mice without Increasing Cancer Incidence. *Aging Cell* **2011**, *10* (4), 604−621.
(47) Ip, F. C. F.; Ng, Y. P.; An, H. J.; Dai, Y.; Pang, H. H.; Hu, Y. Q.; Chin, A. C.; Harley, C. B.; Wong, Y. H.; Ip, N. Y. Cycloastragenol Is a Potent Telomerase Activator in Neuronal Cells: Implications for Depression Management. *Neurosignals* **2014**, *22* (1), 52−63.
(48) Samuel, P.; Tsapekos, M.; de Pedro, N.; Liu, A. G.; Casey Lippmeier, J.; Chen, S. Ergothioneine Mitigates Telomere Shortening under Oxidative Stress Conditions. *J. Diet. Suppl.* **2022**, *19* (2), 212−225.
(49) Tao, L.; Zhang, W.; Zhang, Y.; Zhang, M.; Zhang, Y.; Niu, X.; Zhao, Q.; Liu, Z.; Li, Y.; Diao, A. Caffeine Promotes the Expression of Telomerase Reverse Transcriptase to Regulate Cellular Senescence and Aging. *Food Funct.* **2021**, *12* (7), 2914−2924.
(50) D'Angelo, S. Diet and Aging: The Role of Polyphenol-Rich Diets in Slow down the Shortening of Telomeres: A Review. *Antioxidants (Basel)* **2023**, *12* (12), 2086.
(51) Yabuta, S.; Masaki, M.; Shidoji, Y. Associations of Buccal Cell Telomere Length with Daily Intake of β-Carotene or α-Tocopherol Are Dependent on Carotenoid Metabolism-Related Gene Polymorphisms in Healthy Japanese Adults. *J. Nutr. Health Aging* **2016**, *20* (3), 267−274.
(52) Kadota, K.; Kämäräinen, T.; Sakuma, F.; Ueda, K.; Higashi, K.; Moribe, K.; Uchiyama, H.; Minoura, K.; Tozuka, Y. Unveiling the Flavone-Solubilizing Effects of α-Glucosyl Rutin and Hesperidin: Probing Structural Differences through NMR and SAXS Analyses. *Food Funct.* **2023**, *14* (23), 10493−10505.
(53) Miyake, T.; Kuge, M.; Matsumoto, Y.; Shimada, M. α-Glucosyl-Rutin Activates Immediate Early Genes in Human Induced Pluripotent Stem Cells. *Stem Cell Res.* **2021**, *56*, No. 102511.
(54) Nakata, K.; Morita, N.; Horii, H.; Chubachi, M. Oxidation Intermediates of α-Glucosyl Rutin by Pulse Radiolysis. *Radiat. Phys. Chem. Oxf. Engl. 1993* **1997**, *50* (5), 441−448.
(55) Hashizume, Y.; Tandia, M. The Reduction Impact of Monoglucosyl Rutin on Abdominal Visceral Fat: A Randomized, Placebo-Controlled, Double-Blind, Parallel-Group. *J. Food Sci.* **2020**, *85* (10), 3577−3589.

https://doi.org/10.1021/acsnutrsci.5c00012
ACS Nutr. Sci. XXXX, XXX, XXX−XXX